



Immune response after pig-to-human kidney xenotransplantation: a multimodal phenotyping study

Alexandre Loupy*, Valentin Goutaudier*, Alessia Giarraputo*, Fariza Mezine, Erwan Morgand, Blaise Robin, Karen Khalil, Sapna Mehta, Brendan Keating, Amy Dandro, Anaïs Certain, Pierre-Louis Tharaux, Navneet Narula, Renaud Tissier, Sébastien Giraud, Thierry Hauet, Harvey I Pass, Aurélie Sannier, Ming Wu, Adam Griesemer, David Ayares, Vasishta Tatapudi, Jeffrey Stern, Carmen Lefaucheur, Patrick Bruneval, Massimo Mangiola, Robert A Montgomery

Summary

Background Cross-species immunological incompatibilities have hampered pig-to-human xenotransplantation, but porcine genome engineering recently enabled the first successful experiments. However, little is known about the immune response after the transplantation of pig kidneys to human recipients. We aimed to precisely characterise the early immune responses to the xenotransplantation using a multimodal deep phenotyping approach.

Methods We did a complete phenotyping of two pig kidney xenografts transplanted to decedent humans. We used a multimodal strategy combining morphological evaluation, immunophenotyping (IgM, IgG, C4d, CD68, CD15, NKp46, CD3, CD20, and von Willebrand factor), gene expression profiling, and whole-transcriptome digital spatial profiling and cell deconvolution. Xenografts before implantation, wild-type pig kidney autografts, as well as wild-type, non-transplanted pig kidneys with and without ischaemia-reperfusion were used as controls.

Findings The data collected from xenografts suggested early signs of antibody-mediated rejection, characterised by microvascular inflammation with immune deposits, endothelial cell activation, and positive xenoreactive crossmatches. Capillary inflammation was mainly composed of intravascular CD68⁺ and CD15⁺ innate immune cells, as well as NKp46⁺ cells. Both xenografts showed increased expression of genes biologically related to a humoral response, including monocyte and macrophage activation, natural killer cell burden, endothelial activation, complement activation, and T-cell development. Whole transcriptome digital spatial profiling showed that antibody-mediated injury was mainly located in the glomeruli of the xenografts, with significant enrichment of transcripts associated with monocytes, macrophages, neutrophils, and natural killer cells. This phenotype was not observed in control pig kidney autografts or in ischaemia-reperfusion models.

Interpretation Despite favourable short-term outcomes and absence of hyperacute injuries, our findings suggest that antibody-mediated rejection in pig-to-human kidney xenografts might be occurring. Our results suggest specific therapeutic targets towards the humoral arm of rejection to improve xenotransplantation results.

Funding OrganX and MSD Avenir.

Copyright © 2023 Elsevier Ltd. All rights reserved.

Introduction

Xenotransplantation has the potential to solve worldwide organ shortage by providing an unlimited and renewable source of organs.^{1,2} The use of genetically modified pigs has facilitated this research field by considerably reducing the risk of rejection from preformed xenoantibodies, thus enabling clinically acceptable xenograft survival in non-human primate models.^{3,4}

On the basis of these encouraging results, a pig-to-human kidney xenotransplantation into a heart-beating, brain-dead recipient was performed on Sept 25, 2021, followed by another one on Nov 22, 2021, to assess the safety and efficacy of genetically modified porcine kidneys in humans.⁵ The pigs were bred with a knockout of the alpha-1,3-galactosyltransferase gene to reduce the risk of antibody-mediated rejection secondary to naturally preformed xenoantibodies targeting galactose-alpha-1,3-galactose carbohydrate epitopes,^{6–11} and with a

subcapsular thymic autograft to mitigate the risk of de novo T-cell mediated immune activation.¹² Both xenografts produced urine and remained functional during the 54 h study period, without delayed graft function nor evidence of hyperacute rejection.

This landmark and successful experience gave a considerable boost of hope for the clinical implementation of xenotransplantation. Following this study, the international Banff Foundation for Allograft Pathology, as well as the American Society of Transplantation, the European Society of Transplantation, The Transplantation Society, and the National Institutes of Health appealed to properly characterise xenograft phenotypes to refine next-generation pig models and increase their chance of success in future trials.¹³ We hypothesised that standard histology might not have captured the entire spectrum of immune injuries in these xenografts, and a more precise phenotyping could show rejection processes and tissue

*These authors contributed equally

Université Paris Cité, INSERM U970 PARCC, Paris Institute for Transplantation and Organ Regeneration, Paris, France (Prof A Loupy MD PhD, V Goutaudier MD MSc, A Giarraputo PhD, F Mezine MSc, E Morgan PhD, B Robin MSc, A Certain MSc, A Sannier MD PhD, Prof C Lefaucheur MD PhD, Prof P Bruneval MD); Department of Kidney Transplantation, Necker Hospital, Assistance Publique - Hôpitaux de Paris, Paris, France (Prof A Loupy, V Goutaudier); Cardiovascular Pathology and Pathological Anatomy, Department of Cardiac, Thoracic, Vascular Sciences and Public Health, University of Padua, Padua, Italy (A Giarraputo); NYU Langone Transplant Institute (K Khalil PharmD, S Mehta MD, Prof N Narula MD, Prof H I Pass MD, M Wu MD, A Griesemer MD, V Tatapudi MD, J Stern MD, M Mangiola PhD, Prof R A Montgomery MD PhD) and Department of Pharmacy (K Khalil), NYU Langone Health, New York, NY, USA; Department of Medicine (S Mehta, V Tatapudi), Department of Pathology (Prof N Narula, M Wu, M Mangiola), Department of Cardiothoracic Surgery (Prof H I Pass), and Department of Surgery (Prof H I Pass, A Griesemer, J Stern, Prof R A Montgomery), NYU Grossman School of Medicine, New York, NY, USA; Division of Transplantation, Department of Surgery, Perelman School of Medicine, The University of Pennsylvania, Philadelphia, PA, USA (B Keating PhD); Revivacor, Blacksburg, VA, USA (A Dandro MSc, D Ayares PhD); Paris Cardiovascular Research Center, PARCC, INSERM U970, Université Paris Cité, Paris,

France (P-L Tharaux MD PhD); Ecole Nationale Vétérinaire d'Alfort, IMRB, After ROSC Network, Maisons-Alfort, France (Prof R Tissier DVM PhD); INSERM U1313, IRMETIST, Université de Poitiers et CHU de Poitiers, Poitiers, France (S Giraud PhD, Prof T Hauet MD PhD); Department of Pathology, Bichat Hospital, Assistance Publique - Hôpitaux de Paris, Paris, France (A Sannier); Kidney Transplant Department, Saint-Louis Hospital, Assistance Publique - Hôpitaux de Paris, Paris, France (Prof C Lefaucheur); Department of Pathology, Georges Pompidou European Hospital, Assistance Publique - Hôpitaux de Paris, Paris, France (Prof P Bruneval)

Correspondence to: Prof Alexandre Loupy, Université Paris Cité, INSERM U970 PARCC, Paris Institute for Transplantation and Organ Regeneration, Paris 75015, France alexandre.loupy@inserm.fr

See Online for appendix 1

Research in context

Evidence before this study

Porcine genome engineering has facilitated xenotransplantation by considerably reducing the risk of rejection. The first pig-to-human kidney xenotransplantations were recently performed in brain-dead human recipients. We searched PubMed and MEDLINE on April 18, 2023, using the terms ("kidney" AND "xenotransplantation" AND "pig" AND "human" AND "immune response"), without date or language restrictions. We found that, to date, no peer-reviewed study has investigated the immune response after pig-to-human kidney transplantation using cutting-edge technologies adapted for precision medicine.

Added value of this study

Our study provides the first evidence suggesting antibody-mediated rejection in pig-to-human xenotransplants might be occurring and its underlying biological processes. Using a multimodal strategy combining histo-immunological

damage not readily apparent.

To address this hypothesis, we performed a multimodal deep phenotyping—combining histological and immunological assessments with bulk and spatial transcriptomics—of these two cases of genetically modified pig kidney xenografts transplanted to human recipients. We aimed to precisely decipher and characterise a potential early xenoimmune response and to open avenues and research directions for further refinement of next-generation pig constructs and optimisation of immunosuppressive therapies.

Methods

Study design and participants

We did a multimodal phenotyping study of two pig xenografts transplanted to decedent humans. The multimodal phenotyping was done at the Paris Institute for Transplantation and Organ Regeneration (Paris, France). The ethical foundations of the experimental xenograft transplantation in brain-dead human recipients are in appendix 1 (p 2). The study protocol was approved by the New York University (NYU) Research on Decedents Oversight Committee (registration approval number 002) and written informed consent was obtained from the family of the two brain-dead decedents. The institutional review board of the NYU Grossman School of Medicine approved this study (registration number S19-00192).

Xenotransplantation, xenografts, and control samples

Organ selection and procurement, flow cytometric and real-time complement-dependent cytotoxicity cross-matches, and xenotransplantation procedures have been previously described for the two xenografts analysed in this study⁵ and are summarised in appendix 1 (pp 3–5).

Xenograft samples consisted of wedge biopsy specimens of the two genetically modified renal

phenotyping with bulk and digital spatial transcriptomic profiling, our findings show that xenografts transplanted to humans display antibody-mediated rejection characterised by microvascular inflammation, immune deposits, endothelial cell activation, positive xenoreactive crossmatches and a molecular signature of antibody-mediated injury. Moreover, we highlight that this molecular signature is mainly located in the glomeruli of xenografts, with substantial enrichment of transcripts associated with monocytes, macrophages, neutrophils, and natural killer cells.

Implications of all the available evidence

Our findings suggest that there is a need to better control the humoral arm of rejection to improve xenotransplantation results, and open research directions to optimise immunosuppression strategies and pig constructs in next-generation xenotransplantation clinical trials.

xenografts, sampled 54 h after reperfusion. A multimodal deep phenotyping strategy was applied to each sample, performing both histo-immunological assessment and transcriptomic analyses on the same formalin-fixed and paraffin-embedded tissue to allow a direct comparison between histo-immunological changes and transcriptomic signatures (figure 1). Controls were biopsies from the two genetically modified xenografts obtained before implantation, as well as wild-type, non-transplanted pig kidneys, pig kidney autografts, and non-transplanted pig kidneys with ischaemia-reperfusion injury. Further details on the controls are shown in appendix 1 (pp 6–7, 18–19).

Histological analysis and multi-immunophenotyping

Biopsy specimens were stained with haematoxylin and eosin for histological analysis and by immunohistochemistry for multi-immunophenotyping. C4d, IgM, IgG, monocytes and macrophages, neutrophils, natural killer cells, T cells, B cells, and von Willebrand factor (vWF, a marker of endothelial activation) were stained with anti-C4d, anti-IgM, anti-IgG, anti-CD68, anti-CD15, anti-NKp46, anti-CD3, anti-CD20, and anti-vWF antibodies, respectively. Cross-reactivity of the primary antibodies between species was evaluated with negative human controls (normal peritumoural kidney tissue). All biopsy specimens were assessed by three expert nephropathologists (PB, AS, and VG) who were masked to the clinical and transcriptomic data, and who screened for all lesions that can be observed in pig kidney xenografts,¹⁴ as well as immune deposits, immune cells, and factors involved in biological rejection processes.¹⁵ Immune cell infiltrates were quantified on whole slide images with an end-to-end approach of the HALO AI image analysis software (Indica Labs, Albuquerque, NM, USA) by training built-in segmentation and classification

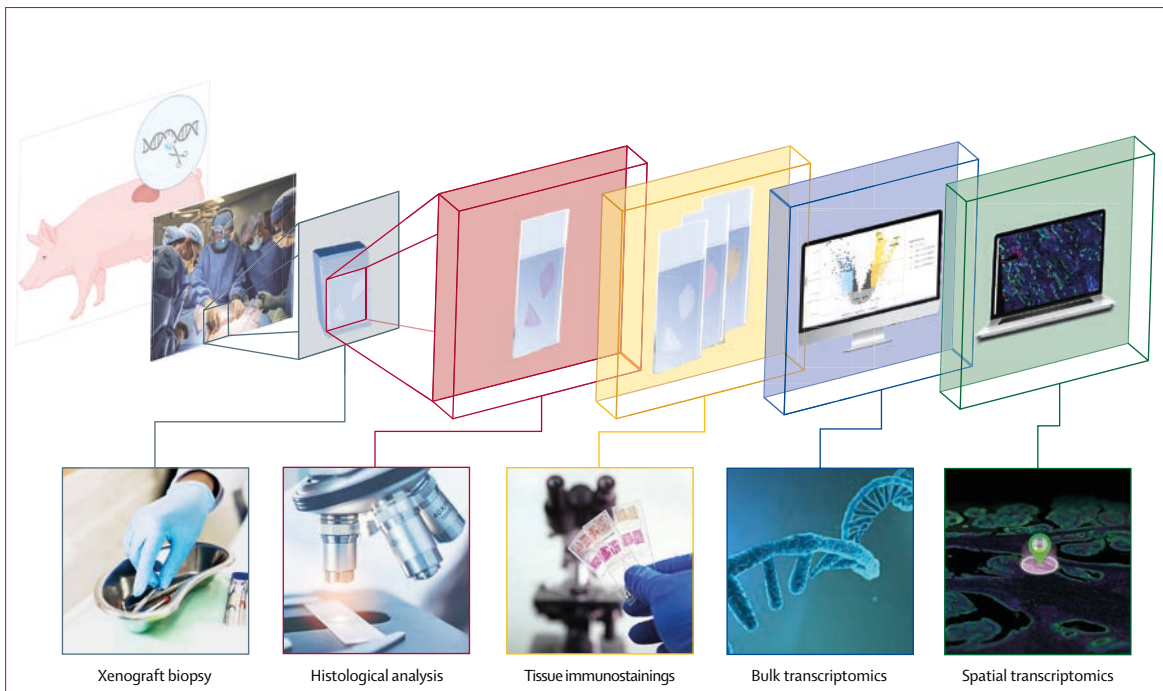


Figure 1: Multimodal deep phenotyping of pig kidney xenografts

We performed a deep phenotyping of xenograft biopsies using a four-step strategy combining a morphological evaluation by histological analysis, immunophenotyping with multiple immunostainings, gene expression profiling with bulk transcriptomics, and whole-transcriptome digital spatial profiling and cell deconvolution. Parts of figure created with BioRender.com.

tools based on convolutional neural networks. Further details are shown in appendix 1 (pp 9, 20–21, 29).

Bulk-tissue transcriptome profiling

Total RNA was isolated from biopsy sections and hybridised with the nCounter Banff Human Organ Transplant panel (NanoString Technologies, Seattle, WA, USA)¹⁶ adapted for porcine–human cross-species analysis. Raw gene count data were analysed using the **nSolver Analysis Software** (version 4.0.70). Quality control metrics¹⁷ ensured the accuracy and reliability of the sequencing data and normalisation was performed using the remove unwanted variation approach.¹⁸ Differential expression analysis was conducted using a Wald test, and p values were adjusted for multiple comparisons using the Benjamini-Hochberg method. Genes with significant changes in expression levels were filtered according to a false discovery rate p value less than 0.05. Significant genes were annotated according to Uniprot¹⁹ and GeneCards²⁰ databases. The molecular signatures were defined according to pathogenesis-based transcripts and the Banff Molecular report,^{15,16,23} defining and sharing common transcripts associated with rejection and immune response in solid organ transplantation. Further details are shown in appendix 1 (pp 10–13, 22–23) and **appendix 2**.

Whole-transcriptome digital spatial profiling

The samples from xenografts before and after implantation and from wild-type, non-transplanted pig

kidney were prepared according to manufacturer's instructions.²¹ Immunofluorescence antibodies were used to identify the renal morphology, including pancytokeratin for epithelial cells, α -smooth muscle actin for fibrogenic cells, calbindin for renal tubules, and Syto 83 (Thermo Fischer Scientific, Waltham, MA, USA) for DNA stain. Two expert nephropathologists (PB and VG) identified eight regions of interest specific to glomeruli and four regions of interest specific to tubulointerstitial compartments in each biopsy.

Whole-transcriptome sequencing was performed using Illumina's i5×i7 dual-indexing system (Illumina, San Diego, CA, USA), following manufacturer's instructions.²² Raw sequencing reads were processed for high quality and reads were aligned to analyse the barcode. Probes designed for human Whole Transcriptome Atlas (NanoString Technologies) were applied and tested against the porcine transcriptome to ensure that the genetic similarity between analogous genes between species was at least 85%.

Differential expression analysis was performed to examine variations between regions of interest selected within glomerular (n=8 per sample) and tubulointerstitial compartments (n=4 per sample). Similarly to bulk-tissue transcriptomic profiling, the annotations of molecular signatures were defined according to pathogenesis based transcripts and the Banff Molecular report.^{15,16,23} A cell deconvolution approach was performed to characterise the phenotypic

For the **nSolver Analysis Software** see <https://nanosttring.com/products/analysis-solutions/ncounter-analysis-solutions/nsolver-data-analysis-support/>

See Online for appendix 2

For **SpatialDecon** see <https://bioconductor.org/packages/release/bioc/html/SpatialDecon.html>

For the **single cell RNA-sequencing datasets** see <https://github.com/Nanostring-Biostats/CellProfileLibrary>

heterogeneity and spatial distribution of cells involved in the xenografts' injuries. Cell type relative abundances were estimated using a constrained log-normal regression (**SpatialDecon**) and cell type specific signatures were derived from 75 available **single-cell RNA-sequencing** datasets. Further details are shown in appendix 1 (pp 14–17, 24–25).

Role of the funding source

The funders of the study had no role in study design, data collection, data analysis, data interpretation, or writing of the report.

Results

The clinical evolution of the two xenografts was previously described.⁵ Briefly, both xenografts began to make urine within moments after perfusion. Over the 54 h of the study, both xenografts continued to produce urine and remained functional, without delayed graft function. The results of crossmatches were also previously described.⁵ Briefly, recipient 1 had low levels of xenoreactive IgM and IgG antibodies, and a minimally positive crossmatch on the complement-dependent cytotoxic assay, which was probably due to IgM and not IgG. However, recipient 2 had moderate levels of xenoreactive IgM and IgG and a positive crossmatch on the complement-dependent cytotoxic assay, which became negative at a serum dilution of 1:64.

At 54 h after reperfusion, both xenografts showed

microvascular inflammation with leukocytes within glomerular capillaries, evocative of ongoing antibody-mediated rejection (figure 2A, sections C1 and D1). Intravascular leukocytes were also present in the peritubular capillaries of xenograft 1 (figure 2A, section C2), but not in xenograft 2 (figure 2A, section D2). Xenograft 1 showed foci of tubulitis, but xenograft 2 did not (figure 2A, sections C3 and D3). Mild tubular injury was observed in both xenografts, being most prominent in xenograft 1 (figure 2A, sections C3 and D3). Arteritis lesions or interstitial haemorrhage and thrombotic microangiopathy were not observed. We did not observe inflammation or tubular injury in wild-type, non-transplanted pig kidneys and xenografts before

implantation (figure 2A, sections A1–3 and B1–3). At 54 h after reperfusion, xenograft 2 showed linear deposits of IgM along glomerular capillaries, but xenograft 1 did not (figure 2B, sections C1 and D1). In both xenografts, we observed linear deposits of IgG along peritubular capillaries (figure 2B, sections C1 and D1). Immunohistochemistry did not show detectable deposition of C4d in peritubular capillaries (figure 2B, sections C3 and D4). We confirmed the presence of glomerulitis, which was mostly composed of innate immune cells (CD68⁺ and CD15⁺ cells; figure 2B, sections C4–5 and D4–5) and rare adaptive immune cells (CD3⁺ and CD20⁺ cells; appendix 1 p 26). NKp46⁺ cells were also observed within the glomerular capillaries of xenograft 2, but not in xenograft 1 (figure 2B,

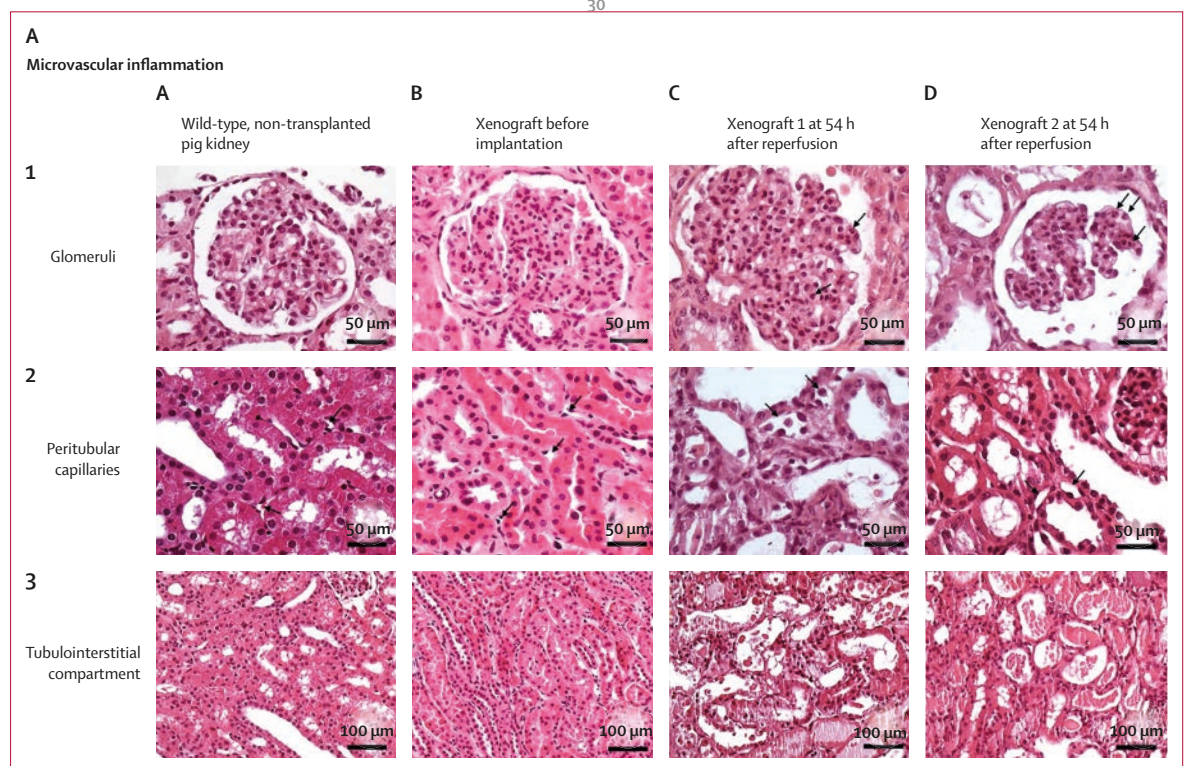


(Figure 2 continues on next page)

sections C7 and D7). Moreover, in xenograft 1 and to a lesser extent in xenograft 2, we observed CD68⁺ cells and rare CD15⁺ cells in the peritubular capillaries (figure 2B, sections C6 and D6). Details on the automated quantification of microvascular inflammation in xenografts are shown in appendix 1 (pp 27–28). Both xenografts showed intense vWF staining in glomerular and peritubular capillaries, indicative of endothelial cell activation (figure 2B, sections C8–9 and D8–9). In wild-type, non-transplanted pig kidneys and xenografts before

implantation, we confirmed the absence of immune deposits and cells (figure 2B, sections A1–7 and B1–7) and observed a weak and expected positive vWF staining in capillaries (figure 2B, sections A8–9 and B8–9). The genes with a significant p value (<0.05 adjusted for false-discovery rate) in the differential gene expression analysis comparing xenografts before and after transplantation are shown in appendix 1 (p 31). We observed increased expression of biologically relevant genes related to antibody-mediated injury (*HLA-A*, *HLA-DRA*, *HLA-DRB1*, *CXCL9*, *HLA-DPA1*, *HLA-DRB3*, *HLA-DPB1*, *WARS*, *GBP1*, and *HLA-B*), endothelial activation (*FGD2*), interferon-gamma (IFN γ) response (*CXCL10*, *B2M*, *IFITM3*, and *GBP5*), natural killer cell burden (*HLA-E* and *FCGR3A/B*), monocyte and macrophage activation (*CD74*, *CD163*, and *CALHM6*), complement activation (*C1QB*), T-cell development (*CD81*), and injury repair response in xenografts at 54 h after reperfusion (figure 3A).

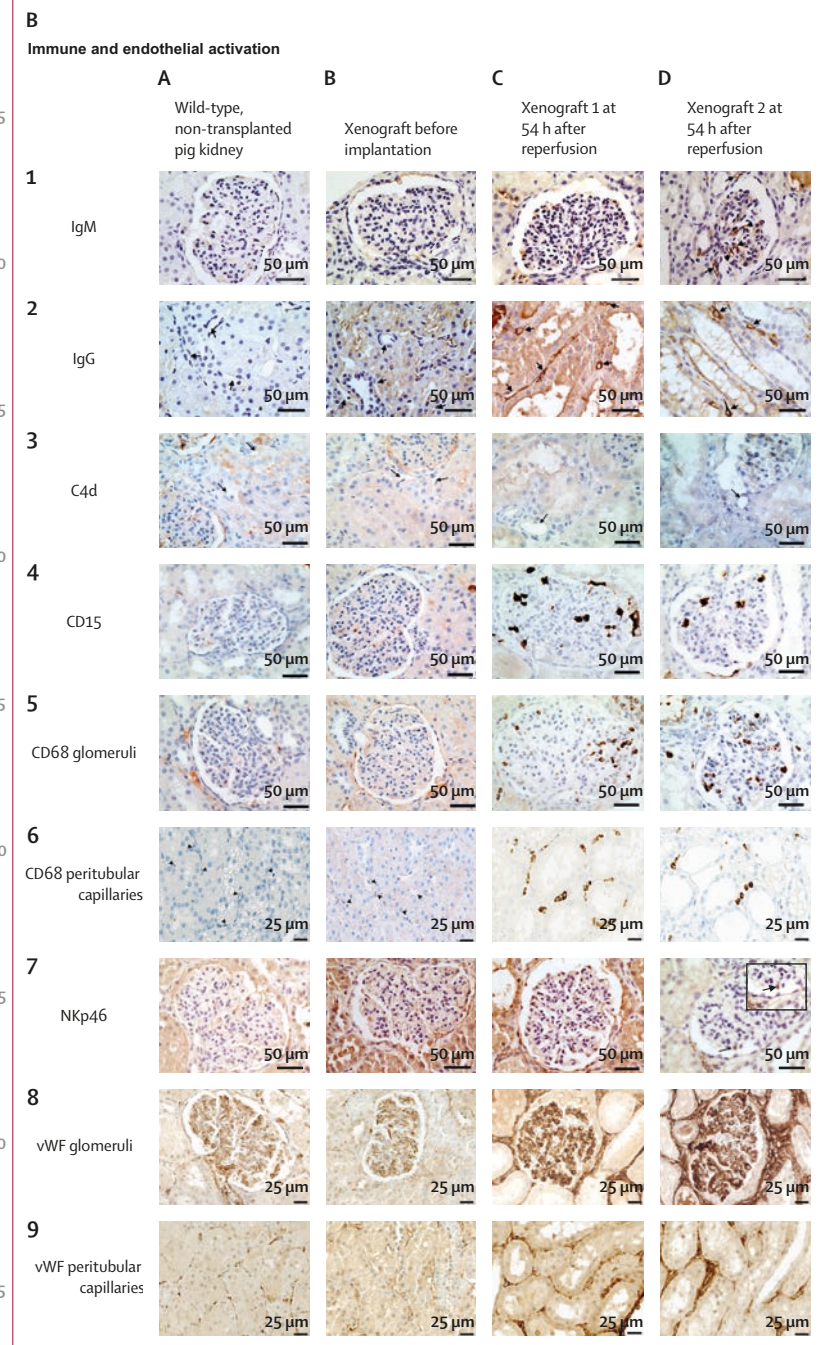
The top 30 ranked differentially expressed genes in xenografts compared with wild-type, non-transplanted pig kidneys are shown in appendix 1 (p 31). We observed increased expression of biologically relevant genes related to antibody-mediated injury (*HLA-A*, *HLA-DRB3*, *HLA-DRA*, *HLA-DRB1*, *HLA-DPB1*, *HLA-DPA1*, *WARS*, and *HLA-B*), IFN γ response (*CXCL9*, *CXCL10*, *B2M*,

GBP1, *IFITM3*, *IFI30*, and *STAT1*), monocyte and macrophage activation (*CD74*, *CALHM6*, *CD68*, and *CD163*), natural killer cell burden (*HLA-E* and *FCGR3A/B*), complement activation (*C1QB* and *C1QA*), T-cell development (*CD81*), and injury repair response in xenografts (figure 3B).

In the differential gene expression analysis comparing xenografts with wild-type pig kidney autografts and non-transplanted pig kidneys with ischaemia-reperfusion, the

Figure 2: Histological and immunological changes occurring in xenografts after transplantation

(A) Haematoxylin and eosin-based evaluation in wild-type, non-transplanted kidney (sections A1–3), xenograft before implantation (sections B1–3), xenograft 1 at 54 h after reperfusion (sections C1–3), and xenograft 2 at 54 h after reperfusion (sections D1–3). Fields representative of glomeruli (row 1), peritubular capillaries (row 2), and tubulointerstitial compartments (row 3) are shown. Black arrows show non-infiltrated peritubular capillaries (sections A2, B2, and D2), infiltrated glomerular capillaries (sections C1 and D1), and infiltrated peritubular capillaries (section C2). (B) Immunohistochemistry-based evaluation for wild-type, non-transplanted kidney (sections A1–9), xenograft before implantation (sections B1–9), xenograft 1 at 54 h after reperfusion (sections C1–9), and xenograft 2 at 54 h after reperfusion (sections D1–9). Fields representative of IgM (row 1), IgG (row 2), C4d (row 3), CD15 (row 4), CD68 (rows 5–6), NKp46 (row 7), and vWF (rows 8–9) stainings are shown. Black arrowheads show linear IgM deposits along glomerular capillaries (section D1). Black arrows show the absence (sections A2 and B2) or presence (section C2 and D2) of linear IgG deposits along peritubular capillaries, the absence of C4d deposit along peritubular capillaries (row 3) and NKp46⁺ cells in glomerular capillaries (section D7).



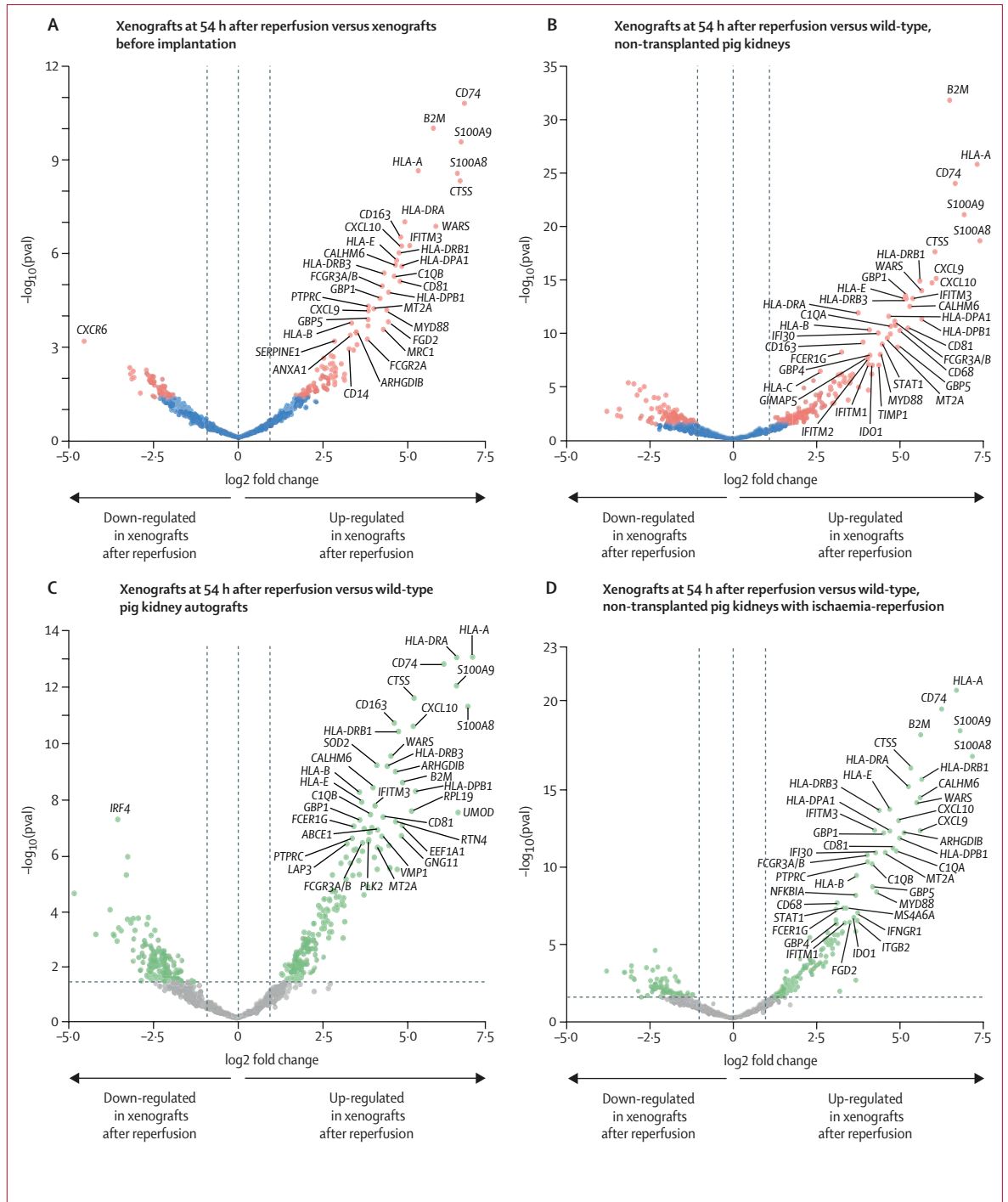


Figure 3: Molecular profiling of xenografts after transplantation

Volcano plots representing the differential gene expression analysis of xenografts at 54 h after reperfusion compared with controls. Dots represent individual genes. The association strength (y-axis) is compared with fold change (x-axis) defined by xenografts versus each contrast of interest: (A) xenografts before implantation, (B) wild-type, non-transplanted pig kidneys, (C) wild-type pig kidney autografts, and (D) wild-type, non-transplanted pig kidneys with ischaemia-reperfusion injury. Significant genes according to p value less than 0.05 are indicated as red dots (A and B) or green dots (C and D).

top 30 ranked differentially expressed genes showed an increased expression of biologically relevant genes related to antibody-mediated and IFN γ response, and injury repair response in the xenografts (figure 3C–D; appendix 1 p 31). In the glomerular regions of interest of xenografts after

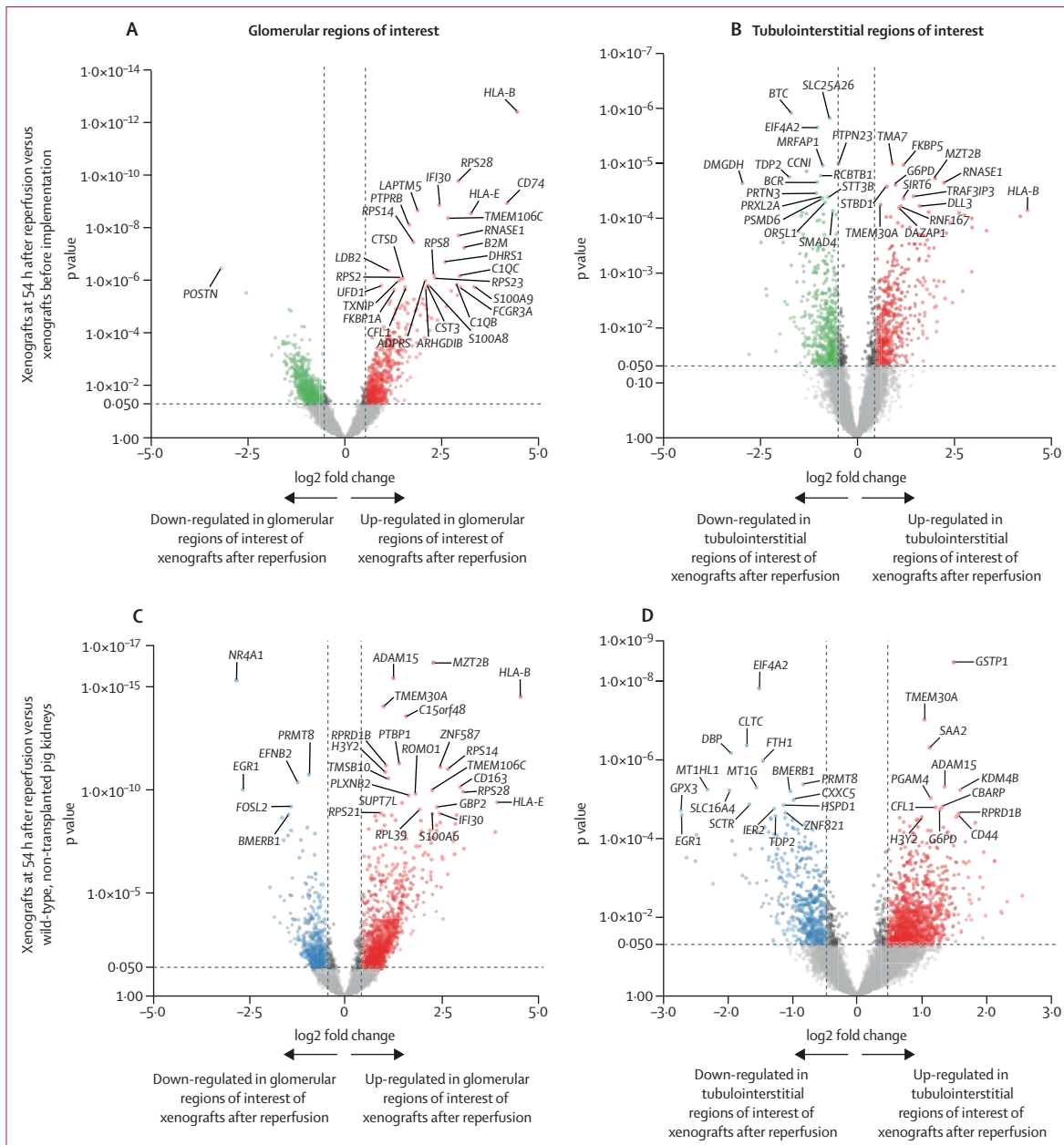


Figure 4: Transcriptional and immune landscape of genetically modified pig kidney xenografts

(A) Volcano plot of the differential gene expression analysis of glomerular regions of interest (eight per biopsy) of xenografts at 54 h after reperfusion compared with xenografts before implantation. Overexpressed genes according to log₂ fold change are indicated in red and underexpressed genes are indicated in green. (B) Volcano plot of the differential gene expression analysis of tubulointerstitial regions of interest (four per biopsy) of xenografts at 54 h after reperfusion compared with xenografts before implantation. Overexpressed genes according to log₂ fold change are indicated in red and underexpressed genes are indicated in green. (C) Volcano plot of the differential gene expression analysis of glomerular regions of interest (eight per biopsy) of xenografts at 54 h after reperfusion compared with wild-type, non-transplanted pig kidneys. Overexpressed genes according to log₂ fold change are indicated in red and underexpressed genes are indicated in blue. (D) Volcano plot of the differential gene expression analysis of tubulointerstitial regions of interest (four per biopsy) of xenografts at 54 h after reperfusion compared with wild-type, non-transplanted pig kidneys. Overexpressed genes according to log₂ fold change are indicated in red and underexpressed genes are indicated in blue. In all panels, dots represent individual genes and the association strength (y-axis) is compared with fold change (x-axis).

reperfusion, we identified an increased expression of key killer cell burden (*FCGR3A* and *HLA-E*), innate immune system (*CST3*, *PTPRB*, and *TXNIP*), injury repair response, tissue damage, and cell processes, compared with the glomerular regions of interest of xenografts before implantation (figure 4A). By contrast, in the

tubulointerstitial regions of interest of the xenografts, we detected few genes related to macrophage activation (*TMEM30A*) and humoral response (*HLA-B*), and an increased expression of non-immune related genes associated with cell processes, signal transduction, and metabolism, compared with the tubulointerstitial regions of interest of xenografts before implantation (figure 4B).

A corresponding spatial molecular pattern was detected for the regions of interest of xenografts after reperfusion compared with the regions of interest of wild-type, non-

transplanted pig kidney, with a molecular signature of antibody-mediated rejection mainly located in the glomeruli (figure 4C–D). In the analysis of the heterogeneity of the xenografts’ molecular-derived immune-cell landscapes, both xenografts showed different immune-cell landscapes and cell populations between the histological compartments (figure 5A). Xenograft 1 showed a heterogeneous cell pattern, with an enrichment of transcripts associated with classical and non-classical monocytes as well as natural killer cells in both glomerular

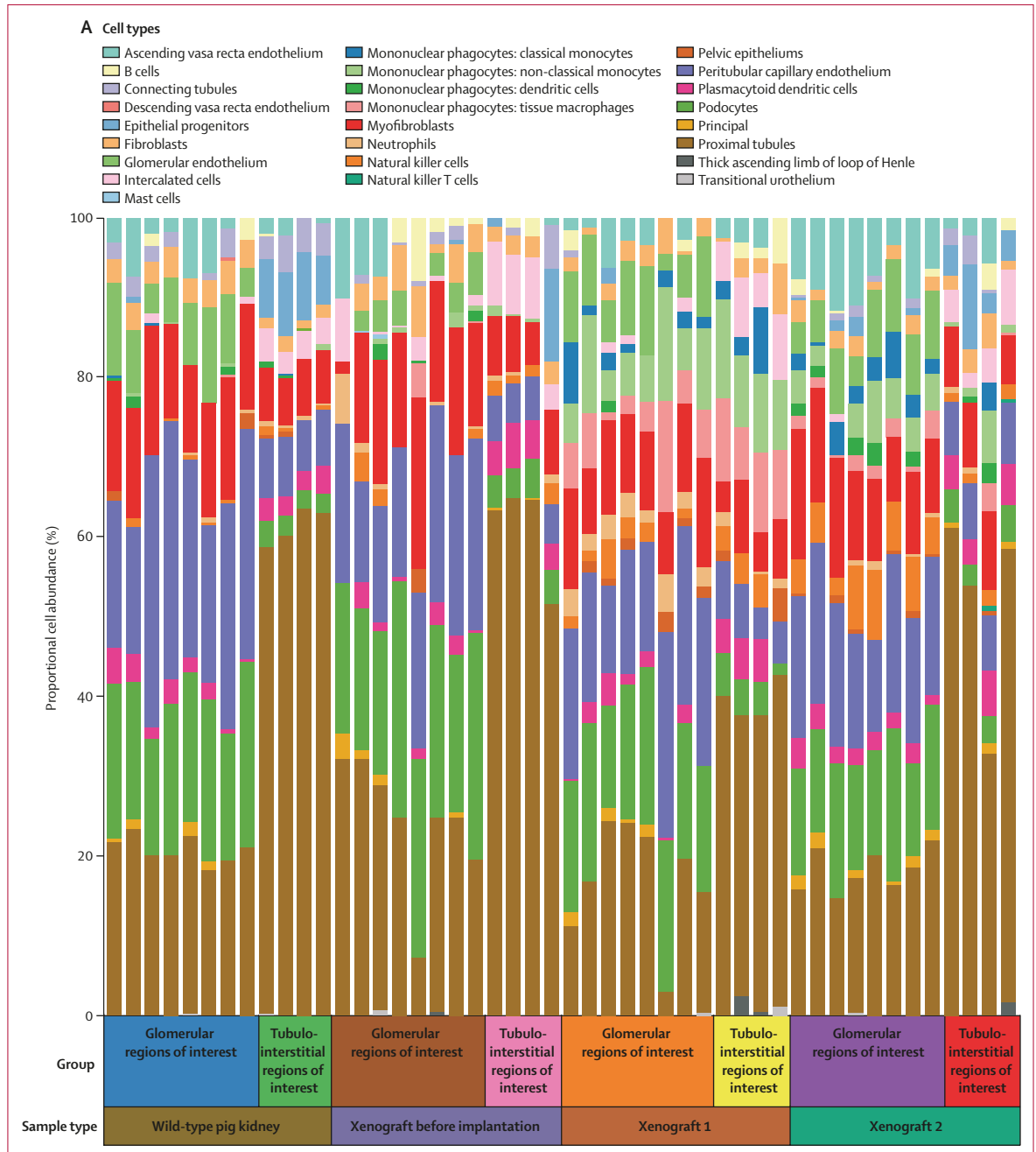


(Figure 5 continues on next page)

1

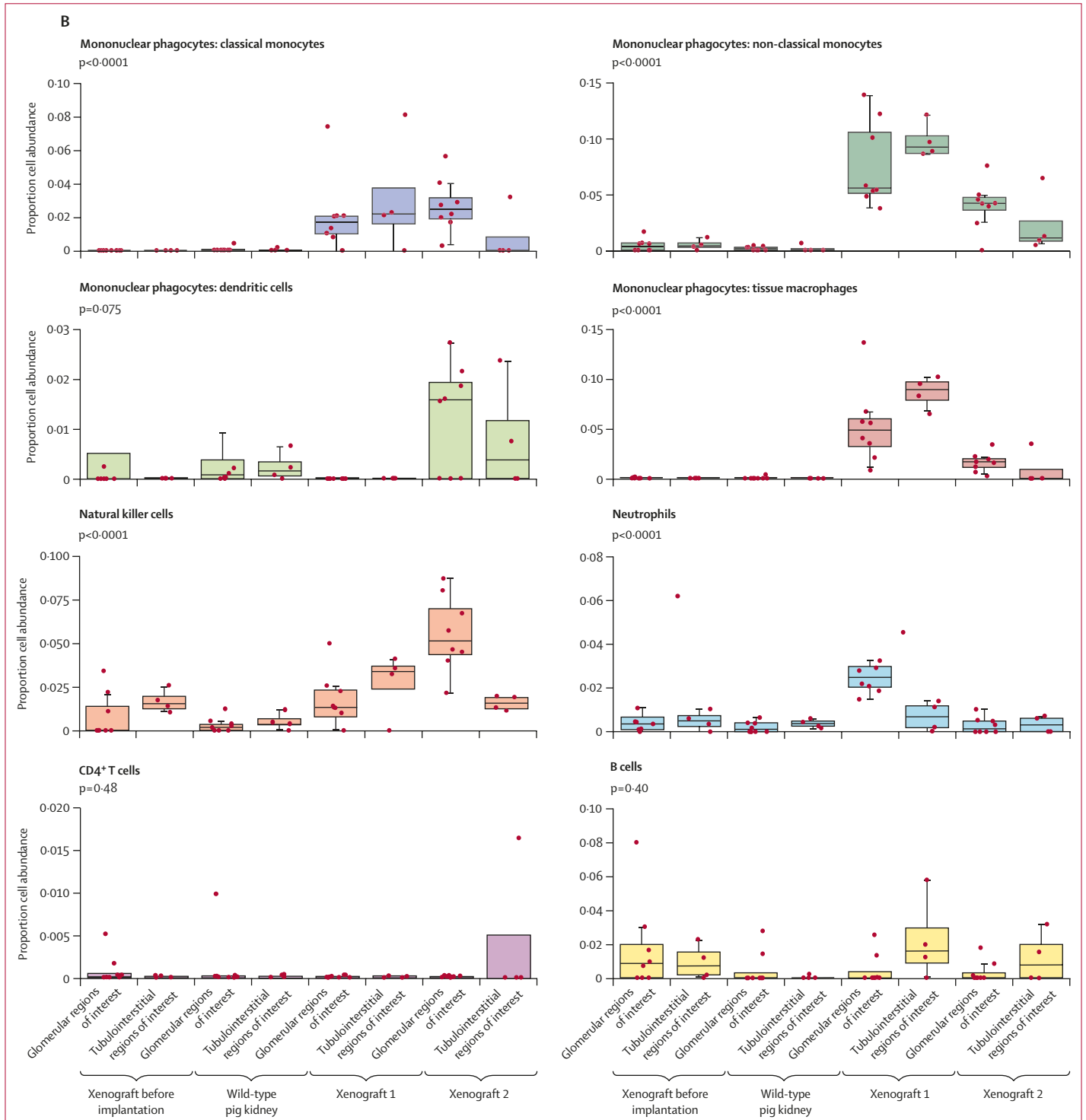


Figure 5: Cell-type spatial profiling of genetically modified pig kidney xenografts

(A) Cell deconvolution output estimating the proportion of each identified cell type in the eight glomerular regions of interest and four tubulointerstitial regions of interest selected for each sample of interest (wild-type, non-transplanted pig kidney; xenograft before implantation; xenograft 1 at 54 h after reperfusion; and xenograft 2 at 54 h after reperfusion). Histograms show the proportional cell abundance referring to the phenotypic heterogeneity and spatial distribution of cells. (B) Boxplots of the average cell abundance identified for the different regions of interest (eight glomerular regions of interest per biopsy and four tubulointerstitial regions of interest per biopsy) in the corresponding samples. Patterns of enrichment are shown as an increase in the average cell abundance, showing range and characteristics of each cell type involved in the immune response.

and tubulointerstitial regions of interest, neutrophils in glomerular regions of interest, and B cells in the tubulointerstitial regions of interest (figure 5B). Macrophage-associated transcripts were enriched in both regions, but were more pronounced in the tubulointerstitial regions of interest (figure 5B). Transcripts associated with dendritic cells and CD4⁺ cells were not detected in either of the regions (figure 5B). In xenograft 2, immune cells were mainly located in the glomerular regions of interest, with an enrichment of transcripts associated with classical and non-classical monocytes, macrophages, natural killer cells, and dendritic cells, as compared with the tubulointerstitial regions of interest. Finally, we observed an enrichment of transcripts related to B cells and CD4⁺ cells in the tubulointerstitial regions of interest, but no enrichment of transcripts associated with neutrophils in both regions (figure 5B).

Discussion

This multimodal deep phenotyping of genetically modified pig kidney xenografts transplanted to brain-dead human recipients showed a pattern of early antibody-mediated rejection with circulating xenoantibodies and immune deposits, confirmed by an increased expression of genes involved in interferon-gamma response, monocyte and macrophage activation, natural killer burden, and endothelial activation. This phenotype occurred predominantly in the glomeruli of the xenografts, and was mainly associated with the involvement of monocytes, macrophages, neutrophils, and natural killer cells.

Our study confirms that the removal of galactose-alpha-1,3-galactose carbohydrate epitopes protects porcine endothelial cells from hyperacute rejection and complement-induced lysis, addressing this previously known issue in xenoimmunity.^{7,9} However, it is important to note that despite this protection, our findings indicate that not all potential xenoimmune-related injuries are fully resolved. Both xenografts showed strong evidence of antibody-mediated rejection: evidence of intravascular leukocytes in glomerular and peritubular capillaries; evidence of current or recent antibody interaction with vascular endothelium, characterised by microvascular inflammation and increased expression of genes associated with antibody-mediated rejection; and serological evidence of circulating donor-specific antibodies in both recipients (ie, xenoantibodies targeting non-galactose-alpha-1,3-galactose antigens). These indolent forms (both xenografts produced urine and recovered renal function) did not show evidence of C4d deposition by immunohistochemistry, suggesting that they were driven by other biological pathways than an activation of the complement cascade.²³ Previous studies in non-human primates have provided valuable insights into immune response after pig kidney xenotransplantation, but the inherent differences between primates and humans necessitated human

studies.² For instance, compared with non-human primates, humans exhibit different immune response, with the involvement of a wider range of immune cells and mediators.⁹ Humans could also display different impacts of porcine genome editing, especially for transgenes that encode human proteins, and have access to different therapeutic options (eg, plasmapheresis are not efficient in non-human primates).⁹

We observed that the effector immune cells of the early rejection process of the xenografts were mainly innate immune cells (macrophages, monocytes, neutrophils, and natural killer cells) and not adaptive T-immune and B-immune cells, in both histological and transcriptomic assessments. The molecular ambience of the interferon-gamma response, monocyte and macrophage activation, and natural killer burden suggested that these effector immune cells were activated and contributed to the endothelial cell activation highlighted in both xenografts by immunophenotyping and transcriptomic profiling. In human kidney transplants, it is now widely recognised that monocytes, macrophages, and natural killer cells are important mediators of antibody-mediated rejection,^{24,25} and that intravascular macrophages without complement deposition primarily represent an indolent and subclinical form of antibody-mediated rejection with potential long-term detrimental consequences for the allograft.²⁶ In the field of xenotransplantation, data from in vitro and preclinical pig-to-non-human primate models also suggest that monocytes, macrophages, and natural killer cells are important effectors of xenograft rejection.²⁷⁻³¹ Interspecies incompatibilities between CD47 and SIRP- α contribute to the rejection of xenogeneic cells by macrophages,³² and antibody-dependent cellular cytotoxicity or direct natural killer cytotoxicity could be implied in human natural killer cell-porcine endothelial cell interactions.³³ Hence, the infiltration of monocytes, macrophages, and natural killer cells in the pig-to-human kidney xenografts might be multifactorial (antibody-dependent cellular cytotoxicity and lack of self-recognition markers).

It is possible that brain death had an influence on the nature of these immune cell infiltrates, as the peripheral cytokines IL-6 and MCP-1 and circulating neutrophils are higher in brain-dead donors than living humans.³⁴ However, in the decedent recipients of this study, these cytokines were initially elevated, but decreased after transplantation,⁵ making it unlikely that cytokines influenced the immune response against the xenografts. Moreover, although the proportion of circulating neutrophils was elevated⁵ and might have led to an increase in intra-graft CD15⁺ cells, the study by Carpenter and colleagues³⁴ showed no significant differences in tissue-resident immune cells between brain-dead donors and controls (particularly in tissues such as the kidney), indicating that the results we observed are probably a reflection of primary immune responses to the xenograft and not an artefact of brain death.

These findings regarding the mechanisms of immune response after pig-to-human kidney xenotransplantation pave the way to optimise next-generation pig constructs in further clinical trials. The thymokidneys transplanted in our model harboured only the alpha-1, 3-galactosyltransferase gene knockout and included a subcapsular thymic autograft. Studies have shown that genetic engineering of human *CD47* and *HLA-E* (encoding a ligand of the inhibitory receptor *CD94/NKG2A*) transgenes in pig organs could protect these organs from macrophage-mediated and natural killer cell-mediated damage.^{35,36} Moreover, the thymic autograft could provide protection from adaptive human immune responses to pig neoantigens and the subsequent interactions with innate immune cells; however, the follow-up period of our study was not sufficient to assess this hypothesis.

The findings of this study also show that biological rejection processes were heterogeneous but mainly located in the glomeruli. Both xenografts showed a microvascular inflammation characteristic of antibody-mediated rejection. In addition, whole-transcriptome spatial profiling showed an increased expression of genes related to immune cells in the glomeruli. Several hypotheses can explain these findings (eg, larger antigenic target for xenoantibody deposition in glomerular capillaries or lack of regulatory membrane proteins), but further investigation is required.³⁷ Interestingly, recipient 2, who had higher levels of xenoantibodies than recipient 1, had more pronounced immunomolecular signs of antibody-mediated injury in the glomeruli.

Combined evidence from our study and previous research also suggests that the xenografts' injuries were mainly associated with an antibody-mediated rejection process rather than ischaemia-reperfusion: (1) the clear molecular signature of antibody-mediated injury compared with pig kidney autografts;¹⁶ (2) the high levels of circulating xeno-antibodies;⁹ (3) the presence of intravascular leukocytes and endothelial cell activation in peritubular capillaries;²⁶ (4) the short duration of cold ischaemia (similar to a living-donor kidney transplantation procedure);³⁸ and (5) the absence of delayed graft function.³⁹

Finally, we acknowledge that our study only involves two xenografts. However, these pig-to-human xenografts are unique. Only one other pig kidney xenograft, with different gene modifications, was transplanted to a brain-dead human recipient, yet did not recover renal function and showed thrombotic microangiopathy.⁴⁰ Moreover, the study follow-up period was not sufficient to assess memory T-cell and B-cell responses or de novo xenoimmune activation (regarding pig neoantigens).⁹ Although we assessed the circulating T cells in the decedent recipients, we did not characterise the circulating innate immune cells (except neutrophils),⁵ so we cannot compare the profiles of circulating and

infiltrative innate immune cells. However, it has been previously shown that there is no difference in the levels of circulating innate immune cells between brain-dead donors and living humans, with the exception of neutrophils.³⁴

In conclusion, using a combination of multidimensional spatial molecular assessment, extensive phenotyping of xenograft biopsies, and characterisation of circulating xenoantibodies, we provide evidence of active antibody-mediated rejection in genetically modified pig kidney xenografts transplanted to human recipients. This pattern was predominantly in the glomeruli of the xenografts, and primarily associated with monocyte and macrophage activation, natural killer cell burden, IFN γ response, and endothelial activation. These results open avenues and research directions to refine next-generation pig gene editing and optimise the control of the humoral harm of rejection in xenotransplantation clinical trials.

Contributors

AL, VG, AGi, FM, EM, BR, AGr, VT, JS, CL, PB, MM, and RAM designed the study and wrote the manuscript. AL, VG, AGi, FM, EM, BR, AS, AGr, CL, PB, MM, and RAM performed the data analysis and interpretation. AL, VG, AGi, FM, EM, BR, KK, SM, BK, AD, AC, P-LT, NN, RT, SG, TH, HIP, AS, MW, DA, AGr, PB, VT, JS, CL, MM, and RAM contributed to the data acquisition. AL, VG, AGi, FM, EM, BR, PB, MM, and RAM accessed and verified the data. AL, VG, AGi, FM, EM, BR, AD, P-LT, RT, SG, TH, AS, MW, DA, AGr, PB, VT, JS, CL, PB, MM, and RAM critically reviewed and revised the manuscript for important intellectual content. All authors had access to all the data in the study and had final responsibility for the decision to submit for publication.

Declaration of interests

AD and DA are employees of Revivacor. All other authors declare no competing interests.

Data sharing

The data and code required to reproduce the figures presented in this study have been deposited in the synapse public repository (<https://doi.org/10.7303/syn49306584>) and are freely available. A sign-in process is required to access the data.

Acknowledgments

We thank Wei Yang and Erin Piazza for their technical assistance and expertise in transcriptomic data analyses, Marion Rabant for providing anti-NKp46 primary antibody, and Julie Piquet from the Alain Carpentier Foundation for providing biopsies of wild-type pig kidneys. We also thank Alton B Farris, Robert B Colvin, Ivy A Rosales, Rex N Smith, and Anthony J Demetris for their constructive discussions and feedback on this work. Academic grant support was provided by the non-profit organisations OrganX and MSD Avenir. VG received grants from the French-Speaking Society of Transplantation and the French Foundation for Medical Research. Research grant support for the decedent studies was provided by Lung Biotechnology, a wholly owned subsidiary of United Therapeutics. The pig kidneys were obtained from Revivacor, a subsidiary of United Therapeutics.

References

- Hryhorowicz M, Zeyland J, Słomski R, Lipiński D. Genetically modified pigs as organ donors for xenotransplantation. *Mol Biotechnol* 2017; **59**: 435–44.
- Montgomery RA, Mehta SA, Parent B, Griesemer A. Next steps for the xenotransplantation of pig organs into humans. *Nat Med* 2022; **28**: 1533–36.
- Wijkstrom M, Iwase H, Paris W, Hara H, Ezzelarab M, Cooper DK. Renal xenotransplantation: experimental progress and clinical prospects. *Kidney Int* 2017; **91**: 790–96.
- Längin M, Mayr T, Reichart B, et al. Consistent success in life-supporting porcine cardiac xenotransplantation. *Nature* 2018; **564**: 430–33.

- 5 Montgomery RA, Stern JM, Lonze BE, et al. Results of two cases of pig-to-human kidney xenotransplantation. *N Engl J Med* 2022; **386**: 1889–98.
- 6 Cooper DKC, Ekser B, Ramsoondar J, Phelps C, Ayares D. The role of genetically engineered pigs in xenotransplantation research. *J Pathol* 2016; **238**: 288–99.
- 7 Galili U. Interaction of the natural anti-Gal antibody with alpha-galactosyl epitopes: a major obstacle for xenotransplantation in humans. *Immunol Today* 1993; **14**: 480–82.
- 8 Galili U, Shohet SB, Kobrin E, Stults CL, Macher BA. Man, apes, and old world monkeys differ from other mammals in the expression of alpha-galactosyl epitopes on nucleated cells. *J Biol Chem* 1988; **263**: 17755–62.
- 9 Griesemer A, Yamada K, Sykes M. Xenotransplantation: immunological hurdles and progress toward tolerance. *Immunol Rev* 2014; **258**: 241–58.
- 10 Cooper DK, Koren E, Oriol R. Oligosaccharides and discordant xenotransplantation. *Immunol Rev* 1994; **141**: 31–58.
- 11 Kolber-Simonds D, Lai L, Watt SR, et al. Production of alpha-1,3-galactosyltransferase null pigs by means of nuclear transfer with fibroblasts bearing loss of heterozygosity mutations. *Proc Natl Acad Sci USA* 2004; **101**: 7335–40.
- 12 Yamada K, Yazawa K, Shimizu A, et al. Marked prolongation of porcine renal xenograft survival in baboons through the use of alpha1,3-galactosyltransferase gene-knockout donors and the cotransplantation of vascularized thymic tissue. *Nat Med* 2005; **11**: 32–34.
- 13 Loupy A, Mengel M, Haas M. Thirty years of the International Banff Classification for Allograft Pathology: the past, present, and future of kidney transplant diagnostics. *Kidney Int* 2022; **101**: 678–91.
- 14 Rosales IA, Colvin RB. The pathology of solid organ xenotransplantation. *Curr Opin Organ Transplant* 2019; **24**: 535–42.
- 15 Loupy A, Lefaucheur C. Antibody-mediated rejection of solid-organ allografts. *N Engl J Med* 2018; **379**: 1150–60.
- 16 Mengel M, Loupy A, Haas M, et al. Banff 2019 Meeting Report: molecular diagnostics in solid organ transplantation-consensus for the Banff Human Organ Transplant (B-HOT) gene panel and open source multicenter validation. *Am J Transplant* 2020; **20**: 2305–17.
- 17 Waggott D, Chu K, Yin S, Wouters BG, Liu FF, Boutros PC. NanoStringNorm: an extensible R package for the pre-processing of NanoString mRNA and miRNA data. *Bioinformatics* 2012; **28**: 1546–48.
- 18 Risso D, Ngai J, Speed TP, Dudoit S. Normalization of RNA-seq data using factor analysis of control genes or samples. *Nat Biotechnol* 2014; **32**: 896–902.
- 19 Bateman A, Martin M-J, Orchard S, et al. UniProt: the universal protein knowledgebase in 2021. *Nucleic Acids Res* 2021; **49**: D480–89.
- 20 Stelzer G, Rosen N, Plaschkes I, et al. The GeneCards Suite: from gene data mining to disease genome sequence analyses. *Curr Protoc Bioinformatics* 2016; **54**: 1.30.1–1.30.33.
- 21 Merritt CR, Ong GT, Church SE, et al. Multiplex digital spatial profiling of proteins and RNA in fixed tissue. *Nat Biotechnol* 2020; **38**: 586–99.
- 22 Zollinger DR, Lingle SE, Sorg K, Beechem JM, Merritt CR. GeoMx™ RNA Assay: high multiplex, digital, spatial analysis of RNA in FFPE tissue. *Methods Mol Biol* 2020; **2148**: 331–45.
- 23 Sis B, Jhangri GS, Bunnag S, Allanach K, Kaplan B, Halloran PF. Endothelial gene expression in kidney transplants with alloantibody indicates antibody-mediated damage despite lack of C4d staining. *Am J Transplant* 2009; **9**: 2312–23.
- 24 Calvani J, Terada M, Lesaffre C, et al. In situ multiplex immunofluorescence analysis of the inflammatory burden in kidney allograft rejection: a new tool to characterize the alloimmune response. *Am J Transplant* 2020; **20**: 942–53.
- 25 Sablik KA, Jordanova ES, Pocorni N, Clahsen-van Groningen MC, Betjes MGH. Immune cell infiltrate in chronic-active antibody-mediated rejection. *Front Immunol* 2020; **10**: 3106.
- 26 Loupy A, Cazes A, Guillemain R, et al. Very late heart transplant rejection is associated with microvascular injury, complement deposition and progression to cardiac allograft vasculopathy. *Am J Transplant* 2011; **11**: 1478–87.
- 27 Lin Y, Vandeputte M, Waer M. Natural killer cell- and macrophage-mediated rejection of concordant xenografts in the absence of T and B cell responses. *J Immunol* 1997; **158**: 5658–67.
- 28 Candinas D, Belliveau S, Koyamada N, et al. T cell independence of macrophage and natural killer cell infiltration, cytokine production, and endothelial activation during delayed xenograft rejection. *Transplantation* 1996; **62**: 1920–27.
- 29 Quan D, Bravery C, Chavez G, et al. Identification, detection, and in vitro characterization of cynomolgus monkey natural killer cells in delayed xenograft rejection of hDAF transgenic porcine renal xenografts. *Transplant Proc* 2000; **32**: 936–37.
- 30 Lu T-Y, Xu XL, Du XG, et al. Advances in innate immunity to overcome immune rejection during xenotransplantation. *Cells* 2022; **11**: 3865.
- 31 Schuurman H-J, Cheng J, Lam T. Pathology of xenograft rejection: a commentary. *Xenotransplantation* 2003; **10**: 293–99.
- 32 Ide K, Wang H, Tahara H, et al. Role for CD47-SIRPalpha signaling in xenograft rejection by macrophages. *Proc Natl Acad Sci USA* 2007; **104**: 5062–66.
- 33 Puga Yung G, Schneider MKJ, Seebach JD. The role of NK cells in pig-to-human xenotransplantation. *J Immunol Res* 2017; **2017**: 4627384.
- 34 Carpenter DJ, Granot T, Matsuoka N, et al. Human immunology studies using organ donors: impact of clinical variations on immune parameters in tissues and circulation. *Am J Transplant* 2018; **18**: 74–88.
- 35 Tena AA, Sachs DH, Mallard C, et al. Prolonged survival of pig skin on baboons after administration of pig cells expressing human CD47. *Transplantation* 2017; **101**: 316–21.
- 36 Weiss EH, Lilienfeld BG, Müller S, et al. HLA-E/human beta2-microglobulin transgenic pigs: protection against xenogeneic human anti-pig natural killer cell cytotoxicity. *Transplantation* 2009; **87**: 35–43.
- 37 Nankivell BJ, P'Ng CH, Shingde M. Glomerular C4d immunoperoxidase in chronic antibody-mediated rejection and transplant glomerulopathy. *Kidney Int Rep* 2022; **7**: 1594–607.
- 38 Ponticelli CE. The impact of cold ischemia time on renal transplant outcome. *Kidney Int* 2015; **87**: 272–75.
- 39 Schröppel B, Legendre C. Delayed kidney graft function: from mechanism to translation. *Kidney Int* 2014; **86**: 251–58.
- 40 Porrett PM, Orandi BJ, Kumar V, et al. First clinical-grade porcine kidney xenotransplant using a human decedent model. *Am J Transplant* 2022; **22**: 1037–53.